Analysis of Prediction Capability of FDS for Response of Thermal Detectors

MORGAN J. HURLEY*
Society of Fire Protection Engineers, Bethesda, MD 20814, USA

ALEX MUNGUIA
The Protection Engineering Group, Duluth, GA 30096, USA

ABSTRACT: Predictions of gas temperature in the fire plume and ceiling jet as well as the response of thermal detectors due to a growing heptane-spray fire were obtained from Fire Dynamics Simulator, version 4 and compared to data from a series of full-scale tests conducted beneath a ceiling suspended in a large facility. This facility consisted of a 36.6×36.6 m compartment with ceiling heights ranging from 3.0 to 12.2 m. Heat release rates followed a modified *t*-squared growth profile. Thermocouples attached to brass disks were used to simulate thermal detectors. Outside the plume centerline, predictions of both gas and disk temperature rise taken together were within a factor of 1.9 of corresponding test data. Although the multiplicative factor of 1.9 was developed by considering all scenarios collectively, a smaller multiplicative factor could have been suggested if some outlying data were excluded. Experimental test data from scenarios that do not correspond to specific configurations of interest could also be excluded, thereby resulting in a multiplicative factor less than the value of 1.9.

KEY WORDS: FDS, DETACT-QS, fire model validation, thermal detectors, growing heptane-spray fire.

INTRODUCTION

IN 2002, THE Society of Fire Protection Engineers (SFPE) published the *Engineering Guide: Evaluation of the Computer Fire Model DETACT-QS* [1]. This guide was the first comprehensive, independently conducted evaluation of a computer fire model ever published.

DETACT-QS [2] is a fire model that estimates the activation time of thermal detectors and sprinklers. DETACT-QS uses correlations developed

*Author to whom correspondence should be addressed. E-mail: mhurley@sfpe.org

1042-3915/10/02 0077–23 $10.00/0 DOI: 10.1177/1042391509360272

SAGE Publications, Los Angeles, London, New Delhi and Singapore

by Alpert [3] to predict the temperature and velocity of fire plumes and ceiling jets resulting from a user-defined fire. Thermal detectors or sprinklers are modeled as a lumped-mass. DETACT-QS solves an ordinary differential equation using an Euler technique. Despite its age, DETACT-QS is still widely used.

Three series of test data were used to evaluate DETACT-QS:

(1) A series of tests conducted at Underwriter's Laboratories that used a heptane spray burner as the fire source with an 'unconfined' ceiling and ceiling heights ranging from 3 to 12 m.
(2) Two tests conducted at FM Global Research that used wood cribs as the fire source.
(3) Tests conducted in a residential-scale room.

SFPE's analysis showed that DETACT-QS predictions were more accurate under some conditions than others. Specifically, SFPE found that as the radial distance of the detector from the plume centerline increased, predictions generally improved. Similarly, predictions generally improved as the response time index (RTI) of thermal detectors increased. Since the scope of the analysis was limited to the evaluation of DETACT-QS, development of better predictive methods was not explored.

More recently, Fire Dynamics Simulator (FDS) [4] has been developed. FDS is a computational fluid dynamics model that permits the discretization of a space into user-defined numbers of grid cells. FDS has quickly become a widely used tool in the fire protection engineering community. FDS models a variety of fire phenomena, including the prediction of sprinkler and thermal detector response.

However, unlike many other computer fire models in existence, FDS uses a technique to model thermal detector response that is much different from that in DETACT-QS. Like DETACT-QS, FDS uses a lumped-mass model of thermal detectors and a numerical technique to determine the thermal response to local gas temperature and velocity. However, FDS determines the temperature and velocity of fire plumes and ceiling jets using a large eddy field modeling technique. Therefore, the conclusions found in [1] are not applicable to FDS.

To determine the capability of FDS to predict thermal detector response, FDS predictions were compared to a subset of data used to evaluate DETACT-QS. Specifically, data from the heptane spray experiments were compared to FDS predictions. FDS version 4.0.6 was used to perform the simulations.

TEST DESCRIPTION

Tests were conducted in a 36.6×36.6 m facility with a smooth, flat, horizontal ceiling that measured 30.5×30.5 m [5]. The ceiling was centered

horizontally within the enclosure, and the height of the ceiling was adjustable. Ventilation exhaust at a rate of 28 m^3/s was provided above the ceiling so that a smoke layer would not form. Make-up air was provided via four 1.5 m diameter ducts located 3 m above the test floor. Tests were conducted with the ceiling positioned at heights of 3.0, 4.6, 6.1, 7.6, 10.7, and 12.2 m. A minimum of two replicate tests were conducted at each ceiling elevation.

The heptane spray burner was located under the center of the moveable ceiling and elevated 0.6 m above the floor. The burner was made using 12 mm diameter piping oriented in a square that measured 1.02 m on a side with two atomizing spray nozzles per side. A diagram of the burner is shown in Figure 1.

Because of the low heptane flow rates used in these tests, only nozzles A, B, D, and G were used in the experiments with ceiling heights of 3.0 and 4.6 m.

The heptane flow rate was controlled manually in an effort to create a growing fire that followed a 'medium' *t*-squared growth curve (fire growth coefficient = 0.01172 kW/s^2). In the tests with ceiling heights of 3.0 m and 4.6 m, fire growth was stopped when heat release rates of 1055 and 2100 kW, respectively, were reached. However, in the other tests, the heptane flow rate was increased throughout the duration of the test.

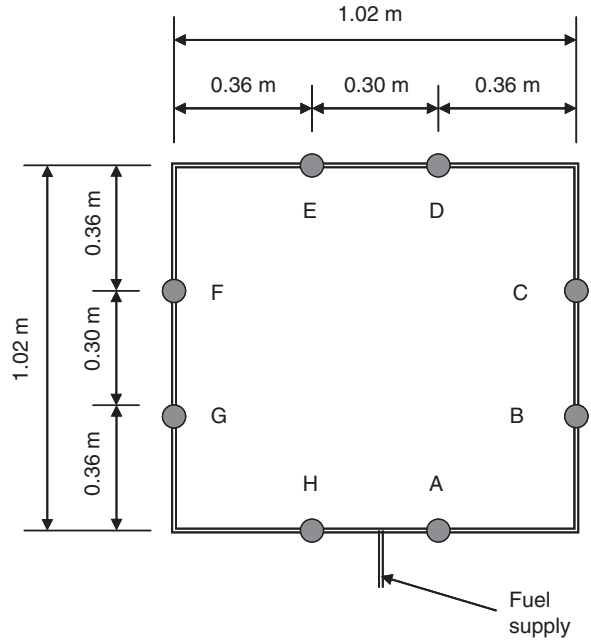

Figure 1. *Burner configuration.*

The flow of heptane to the burner was manually controlled using two float-type flow meters connected in parallel. The first flow meter had a resolution of 0.08 lpm and a range from 0.68 to 9.1 lpm. The second flow meter had a resolution of 1.1 lpm and a range from 0.91 to 11.4 lpm. Given an approximate density and heat of combustion for heptane of 687 kg/m^3 and 44.4 MJ/kg [6], a theoretical heat release rate can be calculated for the fuel as 30.5 MJ/l. Therefore, the measurable flow rate range of the system was able to provide heat release rates ranging from approximately 350 kW $\pm$ 20 kW to 10.4 MW $\pm$ 0.3 MW.

Because of the heptane flow instrumentation limitations, it was not possible to precisely follow the desired medium t-squared growth profile. This was particularly true at the early stages of fire growth where the heptane flow necessary to achieve the desired heat release rate was below the resolution of the flow meters. Therefore, adjustments to the medium growth curve were necessary. A time offset of 200 s was used to increase the minimum fire size.

The initial fire size varied from experiment to experiment due to the limitations of controlling the heptane flow rate and difficulties experienced in igniting the burner at low flow rates. The burner was ignited by four small pilot fires, which were estimated to have a combined heat release rate between 15 and 20 kW. Also, because the flow measurement occurred remotely from the burner, inaccuracies were introduced by fuel line fill time. The heat release rate achieved from the burner was also affected by incomplete combustion in the heptane spray during the early stages of fire growth. This resulted in the creation of pool fires of varying sizes on the floor during the start of the experiments. Based on these factors, and estimations based on the observed fire size, a modification to the medium t-squared growth curve was used to estimate the actual heat release rate achieved.

As the fire size increased, the difficulties with accurately measuring the heptane flow were minimized, and it was possible to follow the medium t-squared growth curve more closely. The equations in Table 1 were used to estimate the heat release rate that was achieved from the burner.

Table 1. Estimated heat release rate from heptane burner.

Time (s)	Heat release rate (kW)
0–40	$\dot{q} = 0.1875(t + 10)^2$
Time > 40	$\dot{q} = 0.0117(t + 160)^2$

Note: The maximum heat release rates in the experiments with 3.0 and 4.6 m ceiling heights were 1055 kW and 2100 kW, respectively.

The ceiling was constructed of 0.6 m × 1.2 m × 16 mm thick UL fire rated ceiling tiles suspended from 38 mm wide steel angle brackets. The reported [5] thermal properties of the ceiling tiles are provided in Table 2.

Instrumentation consisted of thermocouples to measure temperature. Arrays of thermocouples were provided 100 mm below the ceiling at the plume centerline and at radial distances of 2.2 m, 6.5 m, and 10.8 m from the plume centerline. These distances correspond to the radial distances of sprinklers at the corners of squares created by a 3 m × 3 m (10 ft × 10 ft) sprinkler spacing with a fire located at the center of the square (Figure 2).

At each thermocouple array, four thermocouples were provided: a type K inconel sheathed thermocouple, and three thermocouples soldered to 25 mm brass disks to simulate heat detectors. The disks were 25.4 mm in diameter and had thicknesses of 0.41 mm, 3.18 mm, and 6.54 mm. The thermocouples attached to brass disks were determined to have RTIs of 32, 164, and 287 $(\text{m s})^{1/2}$ when tested in accordance with UL 1767 [7]. Other thermocouples

Table 2. Thermal properties of ceiling tiles.

Density	313 kg/m^3
Thermal conductivity	0.0611 W/(m K)
Specific heat	753 J/(kg K)
Thermal diffusivity	2.6 x 10^{-7} m^2/s

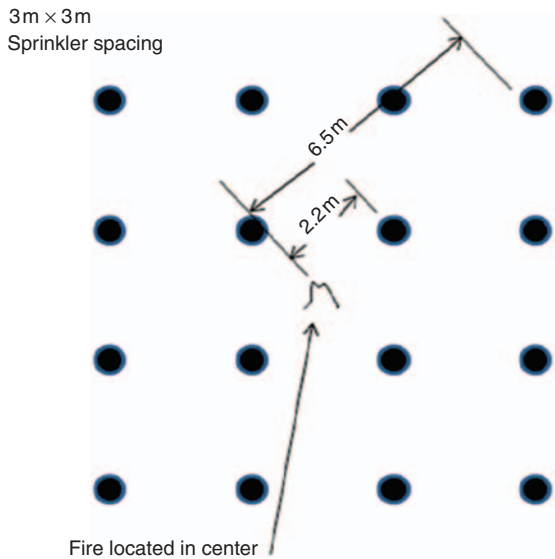

Figure 2. *3 m × 3 m sprinkler spacing. (The color version of this figure is available online.)*

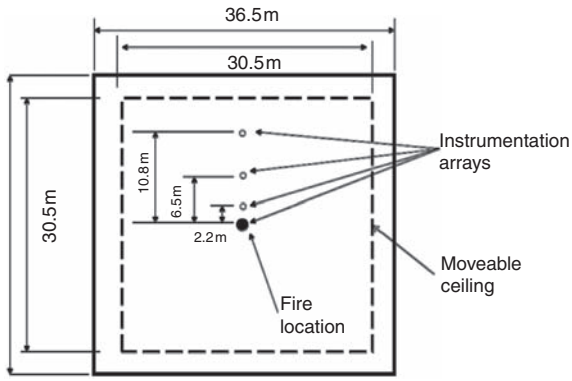

Figure 3. *Reflected plan view of experimental setup.*

were installed but not used in the analysis of FDS. Temperature data were recorded from each thermocouple at 1 s intervals. Figure 3 shows a reflected ceiling plan of the experimental setup.

MODELING APPROACH

FDS input consists of user-prescribed boundary conditions for a user-defined computational domain. Users of the model also specify the grid spacing in each of the Cartesian coordinate directions. Theoretically, as the grid spacing approaches zero, the solutions found should approach the exact solution. However, computational times also increase with the number of grid cells used in a simulation.

Because of the physical size of the experimental facility, it was not possible to run simulations with fine grid resolution within acceptable timeframes. However, it was not necessary to model the entire experimental facility for two reasons: (1) the fire and the instrumentation that were modeled only use a portion of the facility, and (2) because of the physical size of the facility in comparison with the fire size, a significant volume of the space would neither influence, nor be influenced by, the fire.

The space in the vicinity of the fire and the instrumentation was modeled using a multi-block approach. The first block consisted of a 10×10 m computational domain that extended from the floor to the ceiling. The floor was left as the default 'inert' surface, and the ceiling was assigned boundary conditions that corresponded to the material properties of the ceiling tiles used in the experimental setup. The four vertical surfaces of the computational domain were opened to the outside of the computational domain. The grid spacing in the two horizontal directions ('X' and 'Y') were set as 100 mm. The grid spacing in the vertical direction ('Z') was set to be as

close to 100 mm as possible while ensuring that the number of grid cells in the 'Z' direction was only divisible by 2, 3, and/or 5.

A second block was used to simulate the ceiling jet area in the area where the detectors were located. This block abutted the block described above. It also measured 10×10 m, but extended downward from the ceiling to one half of the distance from the floor to the ceiling. A grid spacing of 100 mm was used in the two horizontal directions, and the grid spacing in the vertical direction was identical to that used in the first block. By selecting these grid spacings, the exterior boundaries of the grid cells where the meshes intersected aligned perfectly.

The top of the second mesh was assigned boundary conditions that corresponded to the ceiling tile used in the experimental setup. The remaining five boundaries of the second mesh were opened to the outside of the computational domain. The volume that was above the moveable ceiling, including the exhaust ventilation, was not modeled.

The reaction was set using the parameters for 'heptane' contained in the DATABASE.DATA file that came with version 4 of FDS. In the DATABASE.DATA file, the entry for heptane did not designate a radiative fraction, so FDS used the default value of 0.35.

The burner was modeled as an inert box that measured $1\text{ m} \times 1\text{ m} \times 0.6\text{ m}$. This size was 0.02 m smaller than the burner used in the experiments in each of the horizontal directions. The top of the burner was assigned surface properties that corresponded to the heat release rate of the burner used in the experimental setup. A 'ramp' function was used to match the heat release curve provided in Table 1.

Instrumentation arrays were simulated within FDS by placing 'thermocouples' and 'heat detectors' at locations above the center of the 'burner,' and at radial distances of 2.2, 6.5, and 10.8 m from the center of the burner measured in the 'Y' direction. The instrumentation was placed 0.1 m below the ceiling. Since heat detectors and thermocouples are not 'physical' devices within FDS, at each radial distance the thermocouple and the three heat detectors were located at the same point. Heat detectors were assigned an activation temperature of 1000°C to ensure that a complete record of device temperatures was recorded by FDS.

Figure 4 illustrates how the space was modeled.

The ambient temperature was left as the default value of 20°C. In some experiments the ambient temperature differed from this value by as much as 9°C. It was not possible to determine the ambient temperature in the tests from the recorded data. First, there was no recording in the test report of the time of ignition. Therefore, the ignition time had to be inferred from the test data as the time when a consistent rise in temperature was recorded. This was also complicated by the fact that small pilot flames were used to

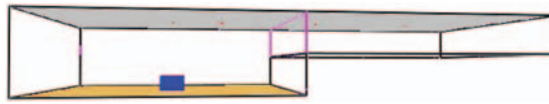

Figure 4. *FDS representation of experimental test facility. (The color version of this figure is available online.)*

ignite the burner, and it was difficult to determine when the temperature rise was caused by the burner and when it was caused by the pilot flames. If the ambient temperature was selected as a time that was clearly before any measurement of temperature rise, the measured temperature at the time of ignition would be much higher than the assumed ambient temperature.

A convergence study was conducted by reducing the grid spacing to approximately 66 mm in each of the three Cartesian coordinate directions for the scenarios with 3.0 m and 6.1 m ceiling heights.

Thermocouple and Brass disk output were imported into a spreadsheet for analysis. FDS 'thermocouple' data exhibited a tremendous amount of scatter. To smooth the thermocouple data, the predicted temperature at each time step was averaged with the predicted temperatures during the preceding four time steps and the subsequent four time steps.

EXPERIMENTAL UNCERTAINTY ANALYSIS

Uncertainty associated with the data used in this analysis comes from three sources: (1) uncertainty in thermocouple temperature measurements, (2) uncertainty in fuel flow measurements, and (3) repeatability uncertainty.

Uncertainty in thermocouple measurements is estimated as $\pm 2.2^{\circ}C$ based on manufacturer's data [8].

The flow meter(s) that were used to measure heptane flows was not reported. Since the flow meter with the greater resolution had a range that was 75% of that of the flow meter with the lesser resolution, it was assumed that the flow meter with the greater resolution was solely used until the heptane flow had reached the limit of the meter's range. This assumption seems reasonable, since the meter with the lesser resolution would not be capable of measuring the flow rates that would occur in the early parts of the experiments.

The resolution of the flow meter with the greatest resolution was 0.08 lpm. Because readings on the flow gage could be made to an accuracy of half the resolution, the estimated uncertainty in flow rate would be ± 0.04 lpm. This corresponds to an uncertainty of ± 20 kW in the heat release rate. The uncertainty in heptane flow during the start-up portion of the test is likely to be greater (and more difficult to quantify). Therefore, the first 100 s of test data were not used. Uncertainty associated with human error in reading the flow meters or in manually controlling the fuel flow rate was not addressed.

To determine the effect on gas temperatures, the uncertainty in heptane flow rate was converted to a temperature value using correlations for fire plume and ceiling jet temperature rise [3]. To provide a conservative estimate, the heptane flow uncertainty was calculated using 20 kW as input. This uncertainty would decrease as the heat release rate of the burner increased.

Repeatability uncertainty was estimated by calculating the standard deviation of temperatures measured in replicate tests. Generally, repeatability uncertainty dominated uncertainty from other sources.

The three types of uncertainty in temperature were combined by using the root-sum-of-squares [9]. For purposes of comparing measured temperatures with FDS predictions, experimental data were reported as a range, which was the average of temperatures from replicate tests plus and minus the combined uncertainty.

An additional source of uncertainty was that the burner may not have been centered directly beneath the thermocouple array that was used to measure temperatures on the plume centerline or there may have been drafts that offset the plume. If this were the case, distances from the plume centerline to the thermocouple arrays that were used to measure temperatures in the ceiling jet region may have differed from that reported. In the test facility, an additional 100 thermocouples were placed 100 mm below the ceiling in a 10×10 square pattern spaced 3 m apart. Ideally, the fire source and the fire plume should have been located below the center of the 10×10 thermocouple array.

To investigate whether the plume was located at the center of the test facility, four thermocouples were selected that were each located at a radial distance of 2.1 m from the burner centerline (the thermocouples formed a $3\,\text{m} \times 3\,\text{m}$ square centered above the burner). It was found that these four ceiling-level thermocouples did not measure the same temperatures. This demonstrates that either the fire source was not centered or there was a draft that offset the plume. Additionally, differences in temperature measurements were systematic; they consistently differed throughout a test. The location of the thermocouples that measured higher temperatures varied from test to test. There was no variation in the location of thermocouples that measured higher temperatures during a single day, but there was a variation from day-to-day. Because of this, it is suspected that the burner assembly was not exactly centered in the test facility or there may have been drafts that offset the plume. However, given that it is not possible to determine exactly where the burner was placed or the magnitude of the drafts that offset the plume, this source of uncertainty was not addressed. There were no visual observations recorded in the test documentation relating to the location of the plume.

The combustion efficiency and the radiative fraction of the heptane were not provided; therefore, it was necessary to use handbook values [6]. How well

these handbook values represented the conditions in the test is unknown, which could introduce another source of unquantifiable uncertainty.

RESULTS

From the grid convergence studies, it was found that grid size independence was achieved for measurements in the ceiling jet region (radial distances of 2.2, 6.5, and 10.8 m from the plume centerline). FDS predictions of temperatures on the plume centerline were found to be sensitive to grid size, and grid size independence was not achieved with the grid spacings that were used in the FDS simulations. Where the plume region ends was not explored in this analysis, since data were only available for detectors located at discrete distances from the plume centerline. However, thermocouples and thermal devices located 2.2 m from the plume centerline did not exhibit the same sensitivity to grid spacing as did thermocouples and thermal detectors located on the plume centerline. Therefore, most results discussed here pertain to locations at radial distances of 2.2 m or greater, which are clearly outside of the plume centerline.

For the test configuration where the ceiling height was 3.0 m, FDS predictions of gas and detector temperature outside of the plume centerline were higher than was measured by sheathed thermocouples (T/C) or thermocouples attached to brass disks (Figure 5). Higher predicted detector temperatures would correspond to prediction of detector activation earlier than would be observed.

At a ceiling height of 4.6 m, FDS predictions were generally within the range of uncertainty outside of the plume centerline (Figure 6). At a radial distance of 2.2 m from the plume centerline, FDS underpredicted the temperature of disks with response time indices of 164 and 287 $(\mathrm{m\,s})^{1/2}$. It should be noted that beginning at a time of 218 s, the measured plume temperatures in one of the experiments (#02169801) began to decrease, eventually differing by $\sim$100°C between the two replicate tests. Additionally, measured plume temperatures differed between replicate tests by as much as 75°C during the first 60 s. Therefore, the experimental data from these tests should be viewed skeptically.

For the tests with 6.1 and 7.6 m ceiling heights, FDS predictions were within the range of experimental uncertainty outside of the plume region, although predictions began to fall below the experimental data for devices with response time indices of 164 and 287 $(\mathrm{m\,s})^{1/2}$ and times greater than 300 s (Figure 7 and Figure 8).

At a ceiling height of 10.7 m, predictions were generally within the range of data outside of the plume centerline, although there were some deviations above and below the data range (Figure 9). As the ceiling height increased to 12.2 m, predictions were within or greater than the range of data outside of the plume centerline (Figure 10).

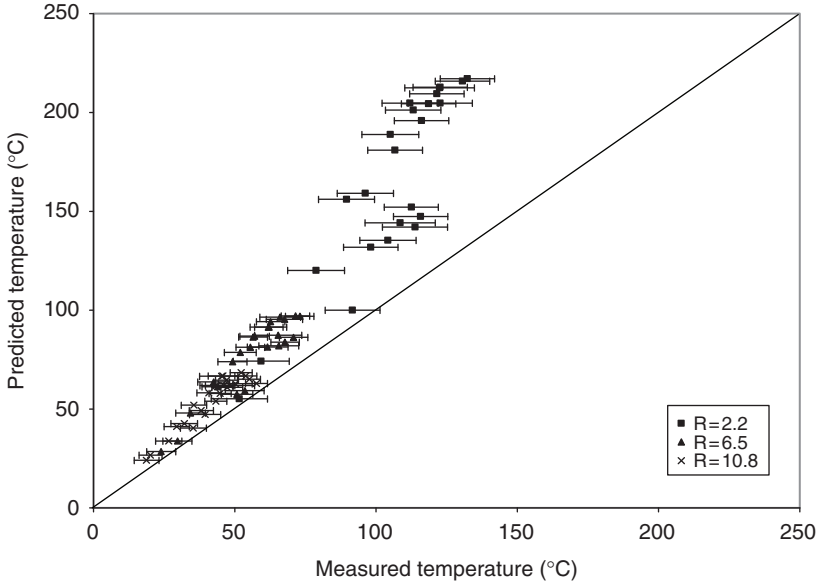

Figure 5. *Comparison of predicted and measured T/C and disk temperatures outside plume centerline for H = 3.0 m.*

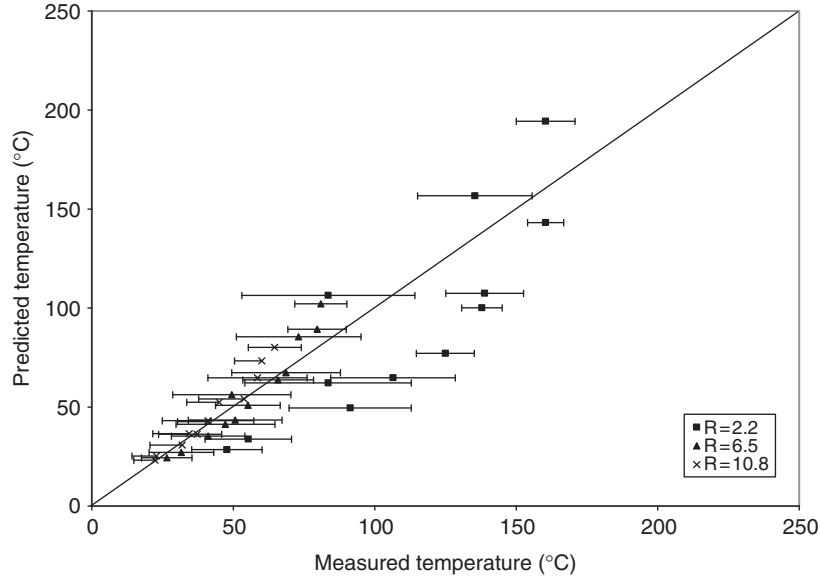

Figure 6. *Comparison of predicted and measured T/C and disk temperatures outside plume centerline for H = 4.6 m.*

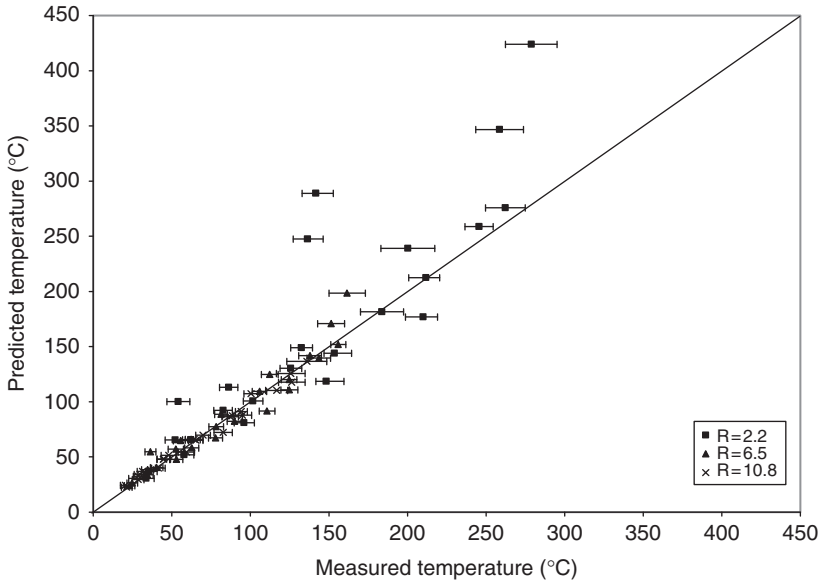

Figure 7. *Comparison of predicted and measured T/C and disk temperatures outside plume centerline for H = 6.1 m.*

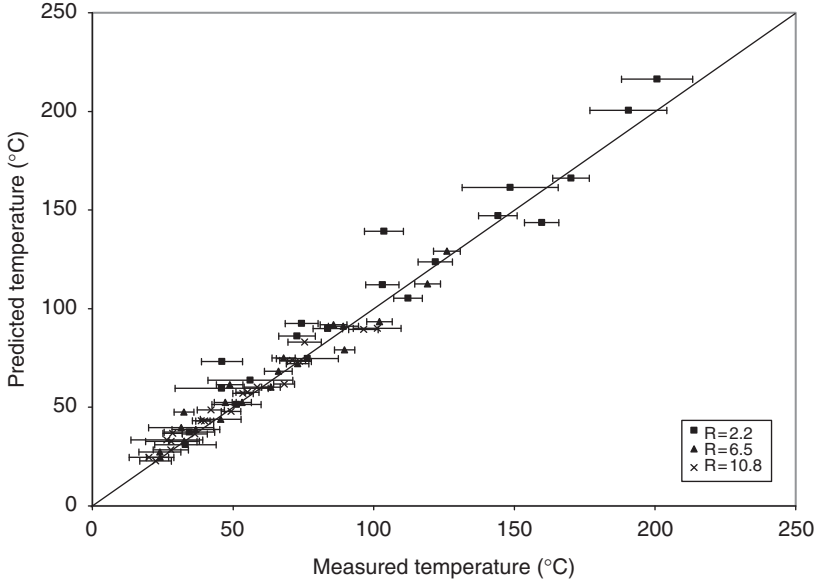

Figure 8. *Comparison of predicted and measured T/C and disk temperatures outside plume centerline for H = 7.6 m.*

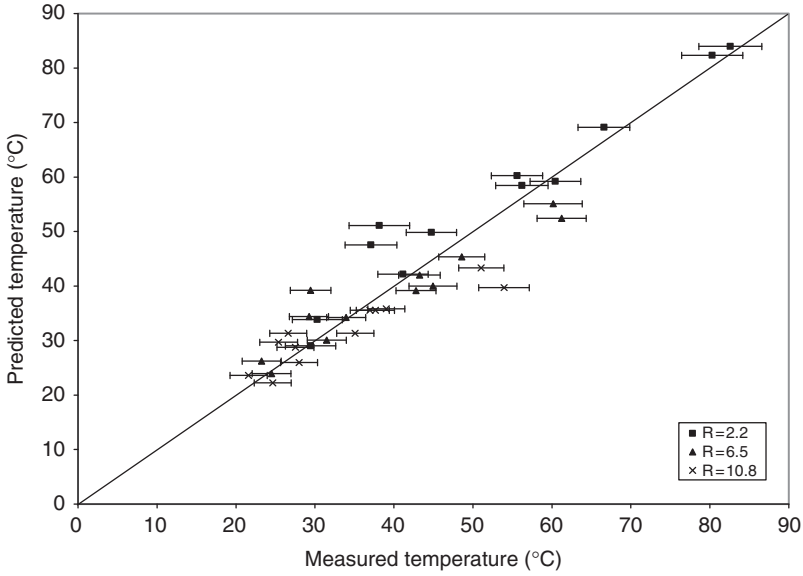

Figure 9. *Comparison of predicted and measured T/C and disk temperatures outside plume centerline for H = 10.7 m.*

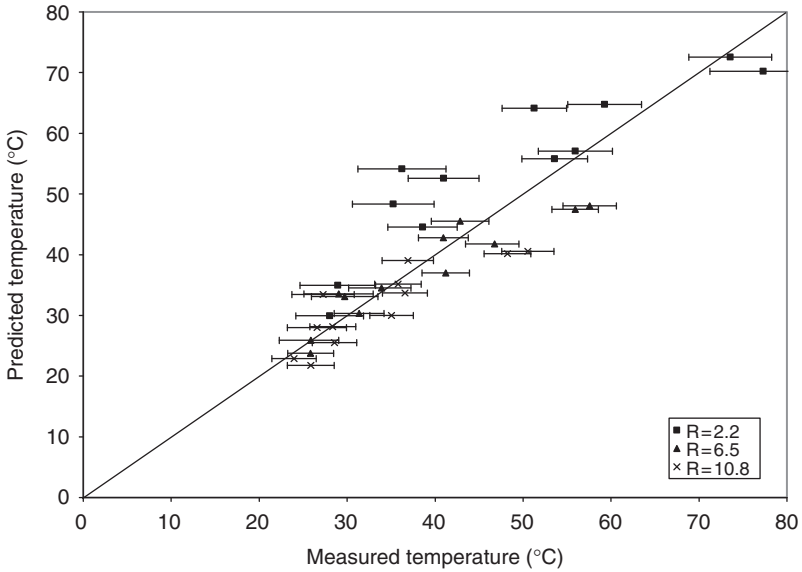

Figure 10. *Comparison of predicted and measured T/C and disk temperatures outside plume centerline for H = 12.2 m.*

ANALYSIS

Overall, predictions outside of the plume centerline were closer to measured temperatures than those nominally on the plume centerline. A part of the reason for this may have been that convergence was not achieved within the plume at the grid spacings (100 mm and 66 mm) used in this study. Given the physical size of the space that was being modeled and the time that it would take to run simulations at finer grid resolutions, further attempts to determine the grid spacing at which convergence would occur within the plume region were not conducted.

Other work has also investigated the capability of FDS to predict plume temperatures [10]. Predictions of plume temperatures were compared to measurements from experiments that used a 0.9 m diameter gas-fired burner. The referenced investigation also found sensitivity to grid spacing, with the best results occurring at a grid spacing of 50 mm. Additional simulations with smaller grid spacings were not conducted to see if grid convergence had occurred. In lieu of conducting additional simulations with further refined grid spacings, the fact that convergence did not occur in the plume region is noted as a limitation of the present study.

To evaluate the results of the analysis for all scenarios, graphs of predicted temperatures versus measured temperatures were prepared. In preparing these graphs, the predicted and measured temperatures were sampled at 100 s intervals. The 100 s sampling rate was selected so that the amount of data in the graphs was manageable and so that data from the first 100 s of the experiments, when there was less certainty in the heat release rate, was excluded. The predicted temperatures and the average of the temperature measurements from replicate experiments at each time interval were plotted. Calculated uncertainty in measured temperatures was displayed using error bars.

Figure 11 contains a plot of data from all ceiling heights, all radial distances, and all types of temperature measurements, both gas and disk. The line drawn in Figure 11 shows perfect agreement. Points plotted above the line are cases where FDS predicted higher temperatures than were measured. Points plotted below the line represent cases where FDS predicted lower temperatures than were measured.

As can be seen in Figure 11, many of the temperature predictions are greater than the measured temperatures. However, most of the points where the greatest over-predictions occur are in the plume centerline. Predictions in this area were more sensitive to grid spacing than in other areas, and grid convergence may not have occurred. Accordingly, measurements and predictions in the plume centerline are not analyzed further and were not used to draw the conclusions noted in this study. Since grid size convergence was likely not achieved in the plume centerline, the

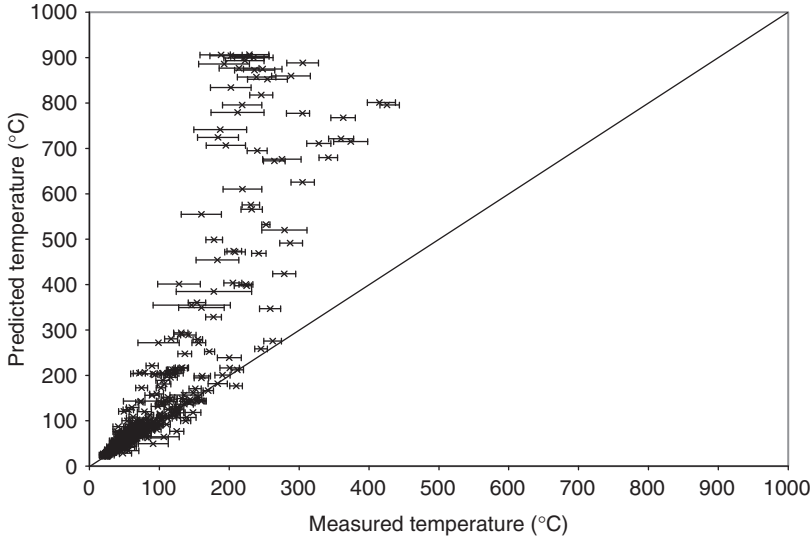

Figure 11. *Comparison of predicted and measured T/C and disk temperatures – both on and outside plume centerline for all ceiling heights.*

findings in this study should not be applied to predictions of temperature or detector response for locations in the plume region.

Figure 12 shows a plot of data from all ceiling heights and all types of temperature measurements that were taken outside of the plume centerline. This includes all radial distances. Figure 13 shows the predicted temperature rise above ambient for all thermocouples and brass disks outside the plume centerline. The temperature rise was calculated by subtracting the ambient temperature from the measured and predicted temperatures of the thermocouples and brass disks.

The lines drawn in Figure 13 have slopes of 1.9 and 1/1.9. This shows that all predictions of temperature rise outside of the plume centerline were within a factor of 1.9 of the measured temperature rise once uncertainty was considered.

It is possible to also look at the influence of ceiling height, radial distance and RTI on the accuracy of predictions. As can be seen in Figures 5–10, predictions more closely match measured temperatures as the ceiling height increases.

Figures 14–17 show comparisons of predicted and measured thermocouple and brass disk temperatures differentiated by the type of sensing device. As can be seen in these figures, the accuracy of predictions is not strongly influenced by the RTI of the thermal device. However, FDS shows less of a tendency to overpredict temperatures as the RTI increases.

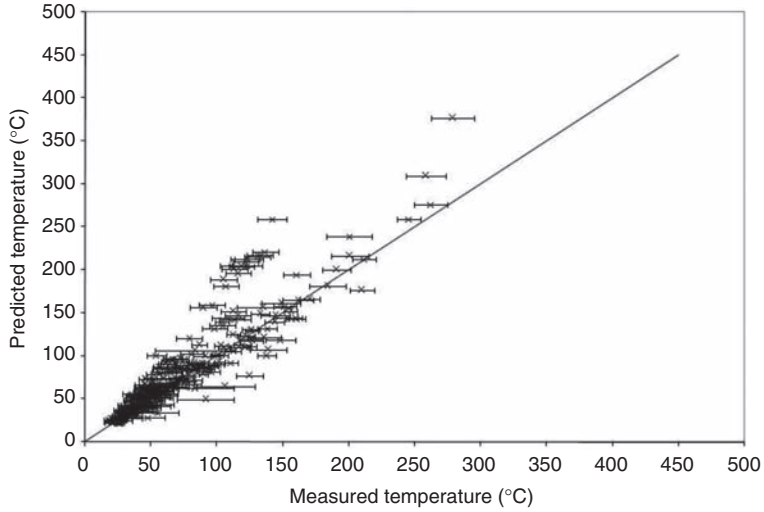

Figure 12. *Comparison of predicted and measured T/C and disk temperatures outside plume centerline for all ceiling heights.*

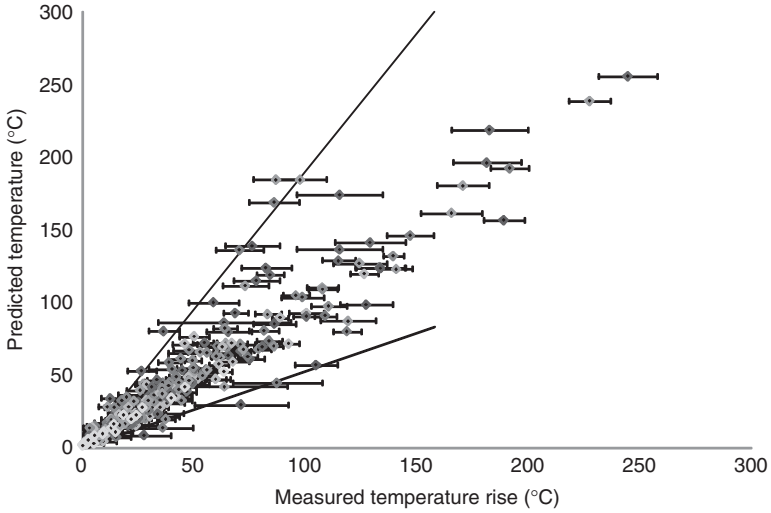

Figure 13. *Comparison of predicted and measured T/C and disk temperature rise above ambient outside plume centerline for all ceiling heights.*

Figures 18–20 show the influence of radial distance on the accuracy of predictions of thermocouple and disk temperature at all ceiling heights. The distance from the plume centerline did not influence the accuracy of FDS predictions.

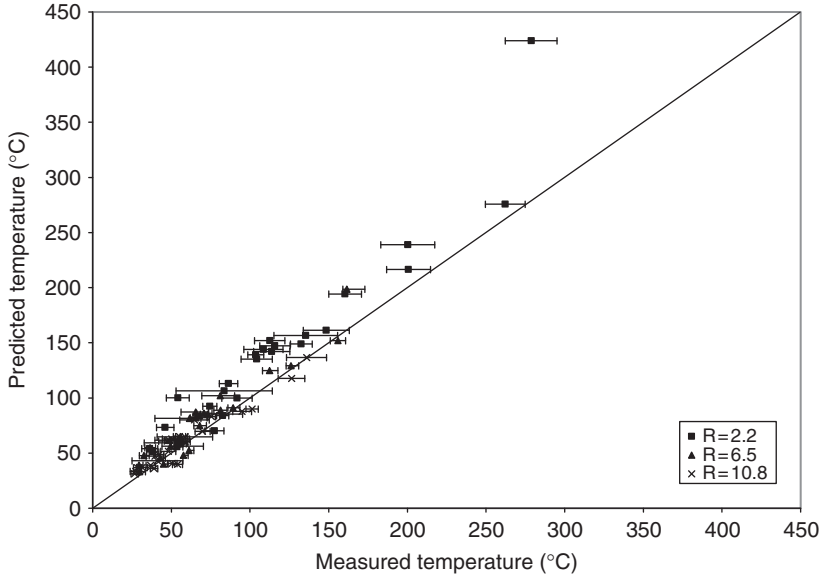

Figure 14. *Comparison of predicted and measured thermocouple (RTI = 0) temperatures outside plume centerline for all ceiling heights.*

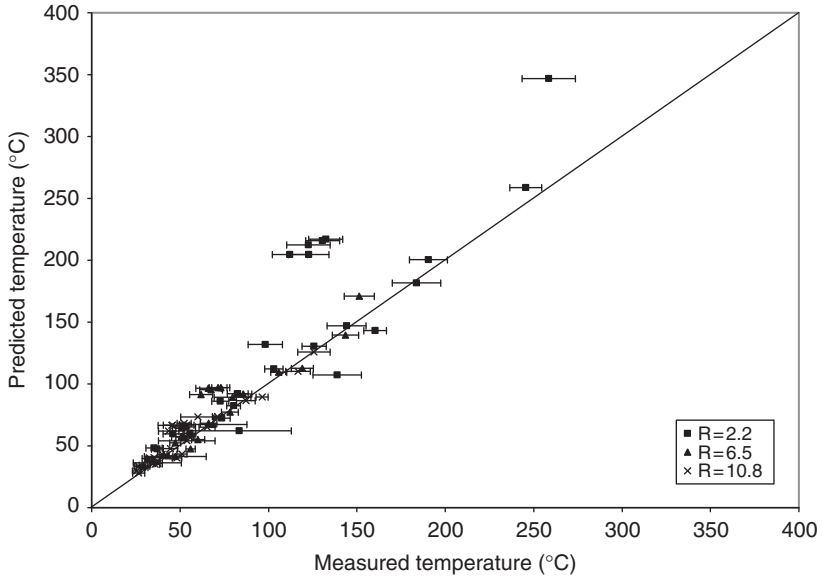

Figure 15. *Comparison of predicted and measured brass disk (RTI = 32 $(m\,s)^{1/2}$) temperatures outside plume centerline for all ceiling heights.*

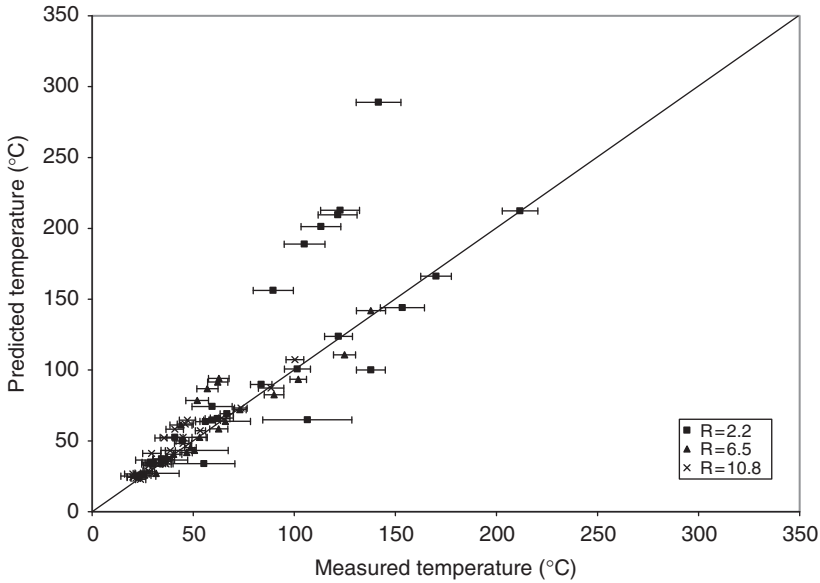

Figure 16. *Comparison of predicted and measured brass disk (RTI = 164 (m s)$^{1/2}$) temperatures outside plume centerline for all ceiling heights.*

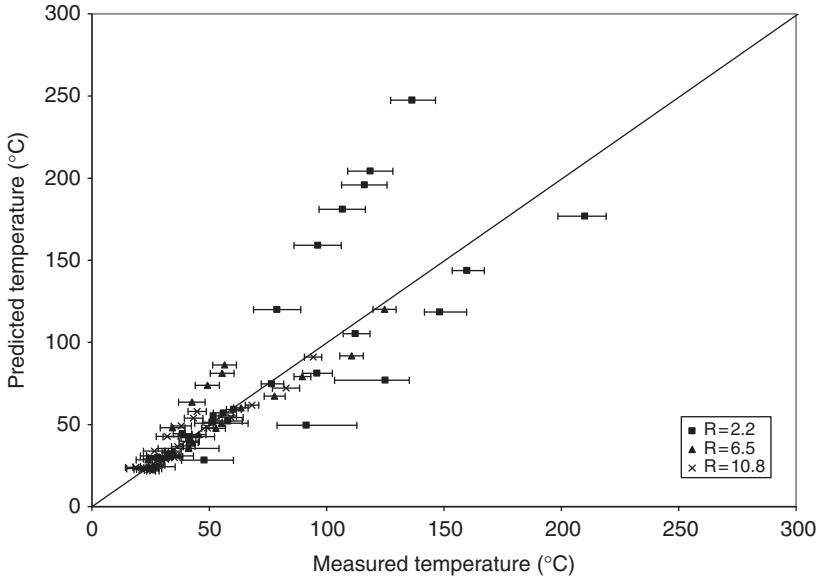

Figure 17. *Comparison of predicted and measured brass disk (RTI = 287 (m s)$^{1/2}$) temperatures outside plume centerline for all ceiling heights.*

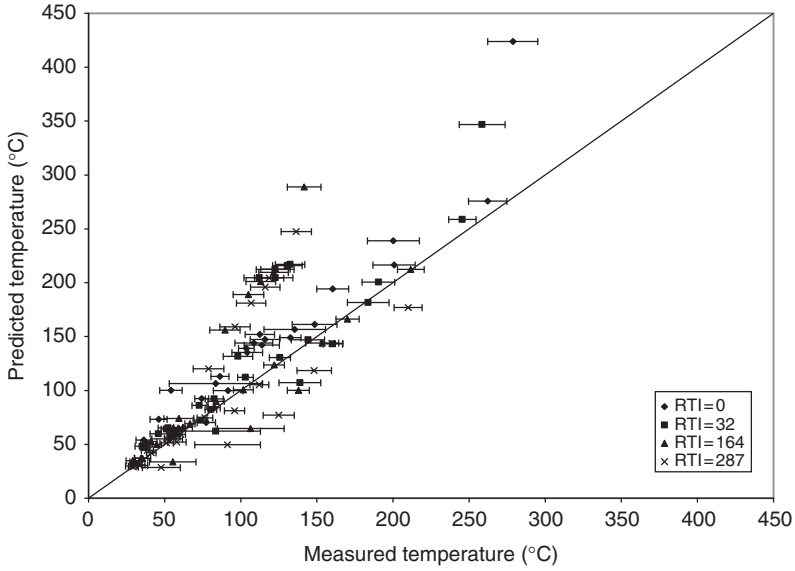

Figure 18. *Comparison of predicted and measured T/C and disk temperatures at R = 2.2 m for all ceiling heights.*

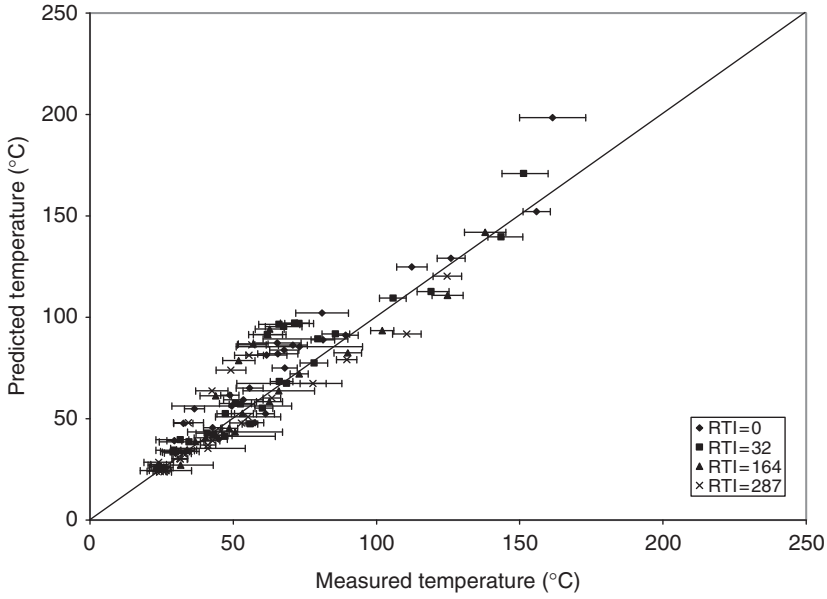

Figure 19. *Comparison of predicted and measured T/C and disk temperatures at R = 6.5 m for all ceiling heights.*

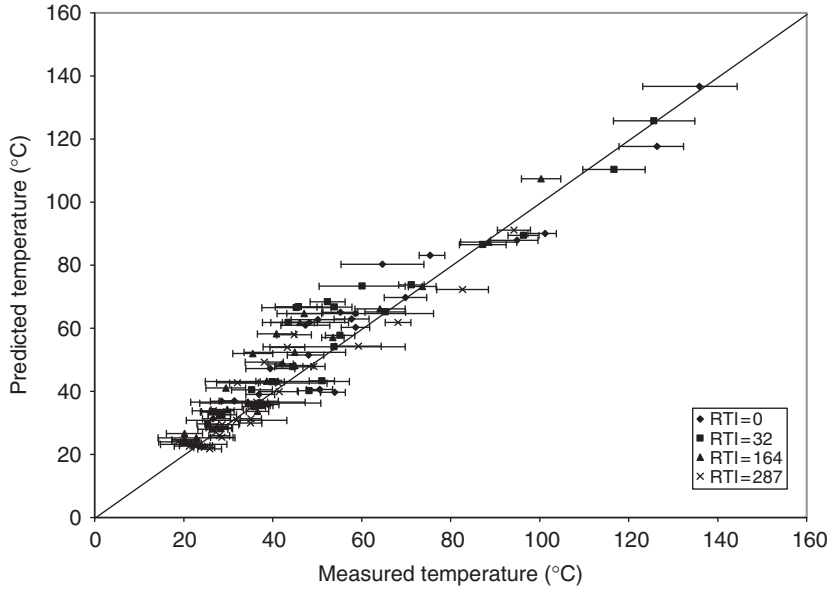

Figure 20. *Comparison of predicted and measured T/C and disk temperatures at R = 10.8 m for all ceiling heights.*

DISCUSSION

Outside of the plume centerline, FDS provides predictions of the increase in gas and thermal detector temperature within a factor of 1.9 of measurements for fires located under an unobstructed ceiling with ceiling heights ranging from 3.0 to 12.2 m.

It is noteworthy that a verification and validation study performed of FDS by NIST [11] found that predictions of ceiling jet temperature rise were accurate to within a factor of 1.16, and predictions of plume temperatures were accurate to within a factor of 1.14. This analysis did not investigate detector response. However, in the NIST analysis, there were data points that were not bounded by these values. The NIST study also recommended a multiplicative factor of 1.2 for predictions of total heat flux. Again, there were data points that were not bounded by this value. A value of approximately 1.7 would be needed to capture all of the data. See Figures 6–11 of reference [11].

All of these multiplicative factors are less than the value of 1.9 that is suggested here. Based on this study, a multiplicative factor of 1.9 was found that bounded at least some portion of the uncertainty range for all of the data used.

When determining sprinkler or detector device response, the fire is typically in a location that would yield a worst-case activation time. If devices are in a square grid, the fire would typically be as far as possible from the nearest device, i.e., a horizontal distance of 0.7 multiplied by the grid spacing. The radial distance of 2.2 m in this study would correspond to a grid spacing of 3.1 m, which is at the lower end of that used in practice. Therefore, results from this investigation should be applicable to most cases of interest despite the inability to draw conclusions regarding devices located on the plume centerline.

Results from this investigation are applicable to the activation of the first sprinkler. The effects of water spray on the operation of subsequent sprinkler activation were not investigated in this study. Similarly, the ability of FDS to model the effect of sprinkler discharge on fire temperatures or fire size was not evaluated. Also, the effect of conduction of heat from sprinklers to sprinkler piping was not considered. FDS does not permit the inclusion of a 'C' factor for heat detectors to account for heat loss to the detector mount, and the thermal devices used in the testing were modeled as heat detectors in FDS. A 'C' factor can be specified for sprinklers in FDS to estimate heat loss to the sprinkler piping.

Since the work described in this article was conducted, a newer version (version 5) of FDS has been released. The underlying hydrodynamic field model used in FDS version 4 calculates plume and ceiling jet temperatures using large eddy simulation. FDS version 5 uses the same hydrodynamic model for smoke and heat transport. The combustion model in FDS version 4 uses a single-step gas reaction. FDS version 5 also includes this single-step reaction as the default, but a multi-step combustion model was also incorporated for use in under-ventilated situations [12]. Because this analysis used a single-step reaction and the experiments were well ventilated, the findings from this study should be applicable to similar analyses using FDS version 5.

CONCLUSION

Outside of the plume centerline, predictions of ceiling jet temperature increase and thermal detector temperature rise were within a factor of 1.9 of measured temperature increases. The multiplicative factor of 1.9 was developed by considering all scenarios collectively. A smaller multiplicative factor could have been suggested if some outlying data were excluded. For specific configurations, experimental test data from scenarios that do not correspond to the configuration of interest could be excluded. In doing so, a smaller multiplicative factor could be appropriately selected.

From a modeling standpoint, 'thermal detectors' could represent the sensing element of sprinklers or heat detectors. For thermal detectors, this factor can be applied by subtracting the ambient temperature from the activation temperature, multiplying this difference by 1.9 and 1/1.9, and then adding the ambient temperature back to these two values. The expected activation time for a given fire should be bounded by predictions from the FDS model using the two temperatures calculated as the activation temperature (for temperatures in °C or K). For example, the expected activation time in a given fire for a heat detector with an activation temperature of 79°C in a room with an ambient temperature of 20°C would be bracketed by the FDS prediction of activation times of detectors with activation temperatures of 51°C and 112°C.

For predictions from the FDS model of temperature in the ceiling jet, the ambient temperature can be subtracted from the predicted temperature, and this temperature rise should be multiplied by 1.9 and 1/1.9, and then the ambient temperature should be added to these two values. The expected temperature of the ceiling jet would be bounded by these two values (again, for temperatures in °C or K).

The full report, which includes FDS input files and graphs showing comparisons of predicted and measured temperatures for each thermocouple type at each ceiling elevation and radial distance, can be found in [13].

ACKNOWLEDGMENTS

The authors express their appreciation to Steve Kerber of NIST for assistance provided in FDS modeling.

REFERENCES

1. Society of Fire Protection Engineers, *Engineering Guide – Evaluation of the Computer Fire Model DETACT-QS*. Bethesda, MD, USA, Society of Fire Protection Engineers, 2002.
2. Evans, D. and Stroup, D., *Methods to Calculate the Response Time of Heat and Smoke Detectors Installed Below Large Unobstructed Ceilings*. NBSIR 85-3167, Gaithersburg, MD USA, National Bureau of Standards, 1985.
3. Alpert, R., "Calculation of Response Time of Ceiling-Mounted Fire Detectors," *Fire Technology*, Vol. 8, No. 3, 1972, pp. 181–195.
4. McGrattan, K. and Forney, G., *Fire Dynamics Simulator (Version 4) User's Guide*. NIST Special Publication 1019, National Institute of Standards and Technology, Gaithersburg, MD USA, 2005.
5. Underwriters Laboratories, *Fire Environment Tests Under Flat Ceilings*. Test Report R18476-96NK37932, Underwriters Laboratories, Northbrook, IL, USA, 1998.

6. DiNenno, P. (ed.), *SFPE Handbook of Fire Protection Engineering*. Appendix C, 3rd Edn, Quincy, MA USA, National Fire Protection Association, 2002.
7. UL 1767, *Standard for Early Suppression Fast Response Sprinklers*. Underwriters laboratories, Northbrook, IL USA, 1995.
8. Omega Engineering Inc., *The Temperature Handbook*, Vol. MM, pp. Z-39–40. CT, USA, Omega Engineering Inc. Stamford, 2000.
9. Taylor, B. and Kuyatt, C., *Guidelines for Evaluating and Expressing the Uncertainty of NIST Measurement Results*. NIST Technical Note 1297. National Institute of Standards and Technology, Gaithersburg, MD USA, 1994.
10. Dreisbach, J. and McGrattan, K., *Verification and Validation of Selected Fire Models for Nuclear Power Plant Applications – Volume 6: Fire Dynamics Simulator*. NUREG-1824 (Draft for Comment). U.S. Nuclear Regulatory Commission & Electric Power Research Institute, Washington, DC USA, 2006.
11. U. S. NRC, *Verification and Validation of Selected Fire Models for Nuclear Power Plan Applications – Volume 7: Fire Dynamics Simulator (FDS)*. NUREG-1824, U.S., Nuclear Regulatory Commission, Washington, DC USA, 2007.
12. McGrattan, K. Hostikka, S. and Floyd, J., *Fire Dynamics Simulator (Version 5) Technical Reference Guide*. NIST Special Publication 1018-5, Gaithersburg, MD USA, National Institute of Standards and Technology, 2009.
13. Hurley, M. and Munguia, A., *Analysis of FDS Thermal Detector Response Prediction Capability*. NIST GCR 09-921. National Institute of Standards and Technology, Gaithersburg, MD USA, 2009.